Electrochemical Corrosion Behaviour of Binary Magnesium Alloys

Hanuma Reddy Tiyyagura[1,5], Balakrishnan Munirathinam[2,6], B. Ratna Sunil[3], Lakshman Neelakantan[2],
Regine Willumeit-Römer[4], Mantravadi Krishna Mohan[1], Vanja Kokol[5]

[1]Department of Metallurgical and Materials Engineering, National Institute of Technology, Warangal, India.
[2]Department of Metallurgical and Materials Engineering, Indian Institute of Technology Madras, Chennai, India.
[3]Department of Mechanical Engineering, Rajiv Gandhi University of Knowledge Technologies (AP-IIIT), Nuzvid, India.
[4]Institute of Material Research, Helmholtz-ZentrumGeesthacht,, Geesthacht, Germany.
[5]Faculty of Mechanical Enginnering,University of Maribor,Slovenia.
[6]Department of Materials Science and Engineering Department, Delft University of Technology, Delft, Netherlands.

Abstract

In this article, electrochemical behavior of pure Mg and as-extruded Mg-5Gd and Mg-4Ag alloys were examined. Electrochemical impedance spectroscopy (EIS) measurements revealed three-time constant behavior at different domains of frequency for all the systems. The charge transfer resistance for Mg-Gd alloy system showed one order higher than that of other systems. Polarization studies indicated that addition of alloying elements shifted the cathodic curve to lower values of current density. Lower corrosion current density is observed for the Mg-Gd system compared to other systems due to alloying addition and grain size effects.

Introduction

Mg and its alloys are the potent third generation metallic materials in the biomedical applications due to their excellent mechanical properties [1–4]. The promising properties such as biodegradability which avoids second surgical procedure to remove the implant in temporary applications and the elastic modulus close to the natural bone that reduces the stress shielding effect made Mg as a viable choice as potential biomaterial [5–8]. However, rapid and uncontrolled corrosion in the physiological environment is the limitation of Mg, that leads to accumulation of hydrogen gas which further decreases the cytocompatibility and results necrosis of tissues [9-10]

Several strategies were adopted to increase the corrosion resistance of magnesium such as developing new alloys, composites and surface coatings [11–15]. The aluminium containing Mg alloys (AZ series) are widely investigated. In recent years, because of toxicity of Aluminium [16], Mg alloys which are free from aluminium were studied for biomedical applications, and promising results were demonstrated [17].Silver is well known for its excellent antibacterial activity in the biomedical field. Mg-4%Ag alloy exhibited profound antibacterial property and corrosion resistance as reported by several investigators [18–20]. On the other hand, rare-earth elements with Mg were found to be suitable for orthopaedic applications [21], particularly, Gd was observed as useful in improving the mechanical properties of Mg alloys [22–24]. From the biomedical perspective, exploring the electrochemical behaviour of these alloys is of cardinal importance. Moreover, no comprehensive report on the electrochemical behavior of these alloys has been reported.

Therefore, in the present work, an extruded Mg-5Gd (wt%) alloy was selected and the electrochemical behavior was assessed and compared with Mg-4%Ag and pure Mg to evaluate the efficacy as a biomaterial.

Experimental

These materials were provided by Helmholtz-Zentrum (HZG), Geesthacht, Germany, and the composition of materials as shown in Table.1 The materials were heat treated and extruded as rods having diameter of 10 mm and height of 1.5 mm, were metallographically polished with different grades of emery sheets followed by polishing by using diamond paste (1-3 µm). The polished specimens were cleaned with ethanol and etched with picric acid reagent, and microstructures were observed using a polarized optical microscope (Leica, Germany). Microhardness measurements were carried outby Vickers indentation method (Omnitech, India) by applying 100 g load for 10 sec. Electrochemical Impedance Spectroscopy (EIS) was performed after attaining stable open circuit potential (OCP) by sweeping the frequency from 0.1 MHz to10 mHz using an AC voltage amplitude of 10 mVrms. Potentiodynamic polarization measurements were carried out in 0.9% NaCl medium by sweeping the potential at a scan rate of 1 mV s^{-1}.

Table 1: Chemical composition and density of Mg, Mg-4Ag and Mg-5Gd

Material	Gd (wt.%)	Ag (wt.%)	Fe (ppm)	Ni (ppm)	Si (ppm)	Mn (ppm)	Co (ppm)	Cu (ppm)	Al (ppm)	Mg
Mg	-	-	46	4	130	334	<1	14	45	bal
Mg-4Ag	-	3.88	58	5	79	51	<1	<10	54	bal
Mg-5Gd	3.99	-	50	6	63	57	<1	<10	41	bal

Corresponding author. Tel. +91 9885673821
E-mail address: mkmohan@nitw.ac.in, vanja.kokol@um.si

Results and Discussion

Figure 1 shows the optical micrographs of pure Mg, Mg-4Ag and Mg-5Gd. The average grain sizes were measured by linear intercept method as 35 ± 10.7, 41.6 ± 11.7 and 19 ± 7.2 µm respectively. From the images, it can be observed that no secondary phase appeared at the grain boundaries in considerable amounts. Numerous twins were observed in Mg and Mg-4Ag, which is common in Mg alloys. However, Mg-5Gd alloy has smaller grains without significant number of twins. The micro hardness was measured as 42.5 ± 2.6, 68.0 ± 4.1 and $69. 2 \pm 3.5$ Hv for Mg, Mg-Ag, and Mg-Gd samples respectively. Compared with pure Mg, both the alloys have shown higher hardness which is presumably due to the alloying effect. Interestingly, the increase in hardness was almost the same for Mg-Ag and Mg-Gd alloys.
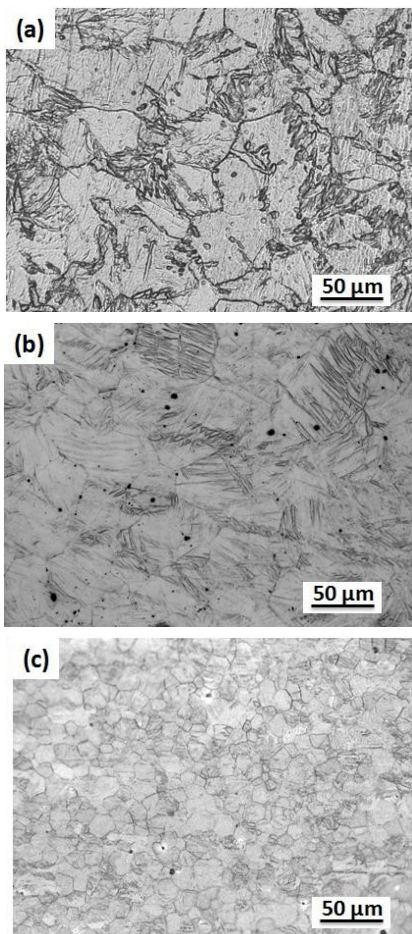

Figure 1: Optical micrographs of (a) pure Mg, (b) Mg-4Ag, and (c) Mg-5Gd

To understand the interfacial properties of these Mg alloys, EIS measurements were performed at 0.9% NaCl conditions under open circuit conditions, as shown in Fig. 2a-b. Bode magnitude and phase plot presented in Fig.2 displays three relaxation features at different domains of frequency. The two relaxation features were observed at high to medium frequencies regions which correspond to the charge transfer reactions in the double layer and to the corrosion products formed due to local environmental changes. At lower frequency region, a drastic reduction in impedance and positive phase shift occurs concomitantly, which can be attributed to the inductive behavior, exhibiting another relaxation feature. It is seen from the Bode magnitude plots that impedance magnitude increases at medium frequency range for Mg-Gd sample, compared to Mg-Ag and Pure Mg.In addition, high impedance behavior of Mg-Gd alloy can be manifested from

the diameter of the capacitive semicircle which is larger than other samples. The loop observed at a lower frequency in Nyquist plot corresponds to the inductive response which can arise due to the adsorption of chloride species or by oxidation of magnesium [25].
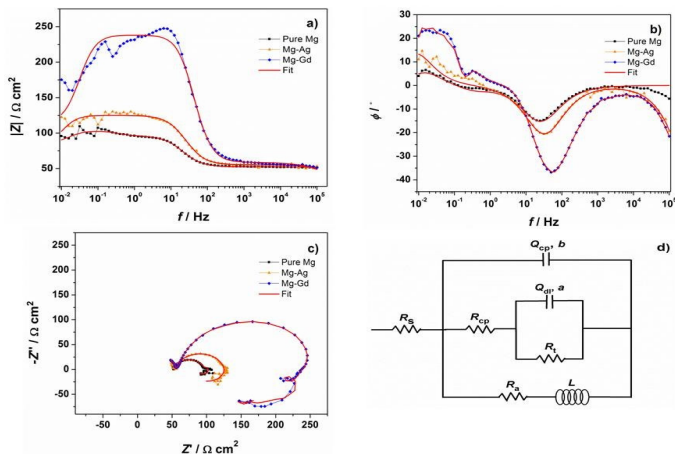

Figure 2: (a) Bode magnitude, (b) Bode phase, (c) Nyquist plots of pure Mg, Mg-4Ag & Mg-5Gd alloy systems, (d) Equivalent circuit used to fit the impedance data.

To model this three relaxation features, an equivalent circuit (Fig.2d) with three-time constants is used [25-26].In this model, R_s represents the solution resistance, Q_{dl} and Q_{cp} represent the constant phase element of electrical double layer and corrosion product film (oxide/hydroxide film) with exponent a and b which is ascribed to the closeness to the capacitive behavior, respectively. To account for the distribution of relaxation times caused by interfacial heterogeneity, Q is employed instead of ideal capacitance. $R_{ct}$is the charge transfer resistance, which accounts for the electron transfer reaction, and R_{ct} is the resistance of the corrosion product formed as a result of cathodic reactions. Under open circuit conditions, the cathodic reaction, namely, hydrogen evolution occurs which increases pH at the vicinity of the electrode. This, in turn, induces alkalinisation, leading to the precipitation of magnesium oxide or gels above the cathodic sites. To account for this, R_{cp} is employed in the circuit. Furthermore, resistance due to air formed oxide/hydroxide (R_a) is included along with inductor (L_a) in series representing the active anodic sites. In principle, inductor offers zero resistance at a lower frequency and higher resistance at a higher frequency. But it is not reasonable to assume that rate of reaction should be frequency dependent. To account for this behavior, R_a is employed, yet from the corrosion perspective, the presence or absence of such resistance is not a concern since it will be short-circuited by an inductor at a lower frequency. The obtained impedance parameters are summarized in Table 2 and the fitting quality was estimated by the chi squared values (χ^2) which were of the order of 10^{-3} to 10^{-4}, suggesting a good fit for the experimental curve recorded. It is clear that a marked change in the resistance values of the Mg alloys is observed. Specifically, Mg-Gd alloys showed higher R_{ct} and R_{cp} values than other samples along with L_a. Higher values of L_a observed for Mg-Gd and Mg-Ag samples indicate that the adsorption of chloride ions in the film is significantly reduced due to the noble nature of these alloying elements. Interestingly, R_a value obtained for all the samples showed values of two orders higher than that of other resistances. As mentioned earlier, these resistance values are not important from the corrosion point of view as this resistance will be short circuited by inductance and assists only in the good fitting of the experimental data.

To gain more insight on the corrosion behavior of these alloys, potentiodynamic polarization measurements (Fig.3) were carried out in 0.9% NaCl medium. It may be observed from these plots

that under cathodic bias, the cathodic curve shifts to lower values of current for Mg-Gd system. Marked change in the slope of the cathodic curve can be attributed to the reduction in the hydrogen evolution reaction. Since corrosion is cathodically controlledin Mg and its alloy system, i_{corr} is estimated using Tafel extrapolation of the cathodic branch to the corrosion potential, E_{corr}. On the other hand, Tafel coefficient is difficult to estimate from the

anodic branches due to the ohmic drop effects taking place during anodic polarization. Close to the corrosion potential and slightly below them i.e. during the initial stage of the cathodic reaction, hydrogen evolved during the reaction increase the pH of the cathodic surface.

Table 2: Impedance parameters extracted from the equivalent circuit fitting

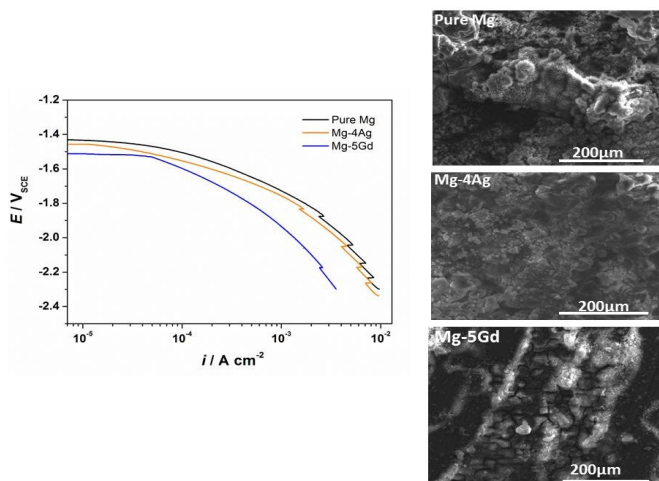| Sample	R_s (Ω cm^2)	Q_{cp} (S s^{a}cm^{-2})	b	R_{cp} (Ω cm^2)	R_a (Ω cm^2)	Q_{dl} (S s^{a}cm^{-2})	a	R_{ct} (Ω cm^2)	L (kH cm^2)	χ^2
Pure Mg	52.29	2.94E-04	0.91	52.34	92.44	5.21E-03	0.89	6.778	1.36	9.34E-04
Mg-4Ag	55.31	2.98E-06	0.92	63.23	207.4	1.53E-04	0.93	69.94	1.87	2.09E-03
Mg-5Gd	53.31	2.07E-06	0.78	76.7	217.6	2.78E-05	0.94	179	4.94	5.85E-03

Figure 3: Polarization curves of pure Mg, Mg-4Ag, and Mg-5Gd recorded in 0.9% NaCl medium (left) b) SEM micrographs recorded after polarization studies (right)

This in turn favours the formation of magnesium oxide/hydroxide formation with chloride ion adsorption in the film which can be manifested from the SEM micrographs (Fig. 3). Lower i_{corr}(5.03 × 10^{-5} A cm^{-2}) is observed for the Mg-Gd system compared to other samples (6.12 × 10^{-5} A cm^{-2} for Mg-Ag; 6.67 × 10^{-5} A cm^{-2} for Mg) due to two inherent features of the system viz., alloying element and grain size. In general, an alloying element like Gd or Ag ions enriched in the film reduces the hydrogen evolution rate significantly leading to the decrease in i_{corr}. Remarkably, smaller grain size which offers more grain boundary area reducesi_{corr}. It is surmised that they act as barriers in blocking the site for the corrosive ions to penetrate inside the film and thereby lower the rate of reaction.

Conclusion

Mg-Gd and Mg-Ag alloys have shown higher hardness in comparison to Mg yet the hardness is more or less the same in both these cases.EIS studies ascertained three relaxation features over the frequency scanned and indicated that the Mg-Gd alloy exhibits higher resistance values than other samples. Polarization studies showed that reduction in hydrogen evolution reaction shifted the cathodic curve to lower values of current density in Mg-Gd system. Lower i_{corr} observed for Mg-alloys which is presumably due to alloying elements and grain size effects. The electrochemical behaviour of Mg-alloys was elucidated and this work could be a way forward to explore the their biological propertiesfor implant applications.

References

1. M. Yazdimamaghani, M. Razavi, D. Vashaee, L. Tayebi, Development and degradation behavior of magnesium scaffolds coated with polycaprolactone for bone tissue engineering, Mater. Lett. 132 (2014) 106–110. doi:10.1016/j.matlet.2014.06.036.
2. H.M. Mousa, A.P. Tiwari, J. Kim, S.P. Adhikari, C.H. Park, C.S. Kim, A novel in situ deposition of hydroxyapatite nanoplates using anodization/hydrothermal process onto magnesium alloy surface towards third generation biomaterials, Mater. Lett. 164 (2016) 144–147. doi:10.1016/j.matlet.2015.10.145.
3. S. Bose, A. Bandyopadhyay, Introduction to Biomaterials, Charact. Biomater. (2013) 1–9. doi:10.1016/B978-0-12-415800-9.00001-2.
4. S. Gaur, S. Nigam, A.S. Khanna, R.K.S. Raman, Silane-Coated Magnesium Implants with Improved In-Vitro Corrosion Resistance and Biocompatibility, Journal of Materials Science & Surface Engg 4 (2016) 415–424.
5. F. Witte, Reprint of: The history of biodegradable magnesium implants: A review., Acta Biomater. 23 Suppl (2015) S28-40. doi:10.1016/j.actbio.2015.07.017.
6. S. Shadanbaz, G.J. Dias, Calcium phosphate coatings on magnesium alloys for biomedical applications: a review., Acta Biomater. 8 (2012) 20–30. doi:10.1016/j.actbio.2011.10.016.
7. F. Witte, N. Hort, C. Vogt, S. Cohen, K.U. Kainer, R. Willumeit, F. Feyerabend, Degradable biomaterials based on magnesium corrosion, Curr. Opin. Solid State Mater. Sci. 12 (2008) 63–72. doi:10.1016/j.cossms.2009.04.001.
8. T.H. Reddy, S. Pal, K.C. Kumar, M.K. Mohan, V. Kokol, Finite element analysis for mechanical response of magnesium foams with regular structure obtained by powder metallurgy method, Procedia Eng. 149 (2016) 425–430. doi:10.1016/j.proeng.2016.06.688.
9. L. Hou, Z. Li, Y. Pan, L. Du, X. Li, Y. Zheng, L. Li, In vitro and in vivo studies on biodegradable magnesium alloy, Prog. Nat. Sci. Mater. Int. 24 (2014) 466–471. doi:10.1016/j.pnsc.2014.09.002.
10. Y. Chen, J. Yan, X. Wang, S. Yu, Z. Wang, X. Zhang, S. Zhang, Y. Zheng, C. Zhao, Q. Zheng, In vivo and in vitro evaluation of effects of Mg-6Zn alloy on apoptosis of common bile duct epithelial cell, Biometals. 27 (2014) 1217–1230. doi:10.1007/s10534-014-9784-x.
11. N.T. Kirkland, N. Birbilis, Magnesium Biomaterials, (2014) 132. doi:10.1007/978-3-319-02123-2.
12. H. Hornberger, S. Virtanen, A.R. Boccaccini, Biomedical coatings on magnesium alloys - A review, Acta Biomater. 8 (2012) 2442–2455. doi:10.1016/j.actbio.2012.04.012.
13. B. Ratna Sunil, C. Ganapathy, T.S. Sampath Kumar, U. Chakkingal, Processing and mechanical behavior of lamellar structured degradable magnesium-hydroxyapatite implants, J. Mech. Behav. Biomed. Mater. 40 (2014) 178–189. doi:10.1016/j.jmbbm.2014.08.016.
14. B. Ratna Sunil, T.S. Sampath Kumar, U. Chakkingal, V. Nandakumar, M. Doble, Friction stir processing of magnesium-nanohydroxyapatite composites with controlled in vitro degradation behavior., Mater. Sci. Eng. C. Mater. Biol. Appl. 39 (2014) 315–24. doi:10.1016/j.msec.2014.03.004.

15. H. Reddy Tiyyagura, R. Rudolf, S. Gorgieva, R. Fuchs-Godec, V.R. Boyapati, K.M. Mantravadi, V. Kokol, The chitosan coating and processing effect on the physiological corrosion behaviour of porous magnesium monoliths, Prog. Org. Coatings. 99 (2016) 147–156. doi:10.1016/j.porgcoat.2016.05.019.

16. R. Walter, M.B. Kannan, In-vitro degradation behaviour of WE54 magnesium alloy in simulated body fluid, Mater. Lett. 65 (2011) 748–750. doi:10.1016/j.matlet.2010.11.051.

17. M.B. Kannan, W. Dietzel, C. Blawert, A. Atrens, P. Lyon, Stress corrosion cracking of rare-earth containing magnesium alloys ZE41, QE22 and Elektron 21 (EV31A) compared with AZ80, Mater. Sci. Eng. A. 480 (2008) 529–539.

18. D. Tie, F. Feyerabend, N. Hort, D. Hoeche, K.U. Kainer, R. Willumeit, W.D. Mueller, In vitro mechanical and corrosion properties of biodegradable Mg-Ag alloys, Mater. Corros. 65 (2014) 569–576. doi:10.1002/maco.201206903.

19. I. Marco, F. Feyerabend, R. Willumeit-Römer, O. Van der Biest, Influence of Testing Environment on the Degradation Behavior of Magnesium Alloys for Bioabsorbable Implants, TMS2015 Suppl. Proc. (2015) 497–506. doi:10.1002/9781119093466.ch63.

20. D. Tie, F. Feyerabend, W.D. Müller, R. Schade, K. Liefeith, K.U. Kainer, R. Willumeit, Antibacterial biodegradable Mg-Ag alloys, Eur. Cells Mater. 25 (2012) 284–298.

21. X. Zhang, Y. Wu, Y. Xue, Z. Wang, L. Yang, Biocorrosion behavior and cytotoxicity of a Mg–Gd–Zn–Zr alloy with long period stacking ordered structure, Mater. Lett. 86 (2012) 42–45. doi:10.1016/j.matlet.2012.07.030.

22. Q. Peng, X. Hou, L. Wang, Y. Wu, Z. Cao, L. Wang, Microstructure and mechanical properties of high performance Mg–Gd based alloys, Mater. Des. 30 (2009) 292–296. doi:10.1016/j.matdes.2008.04.069.

23. J. Kubásek, D. Vojtěch, Structural and corrosion characterization of biodegradable Mg-RE (RE=Gd, Y, Nd) alloys, Trans. Nonferrous Met. Soc. China (English Ed. 23 (2013) 1215–1225. doi:10.1016/S1003-6326(13)62586-8.

24. A. Srinivasan, C. Blawert, Y. Huang, C.L. Mendis, K.U. Kainer, N. Hort, Corrosion behavior of Mg–Gd–Zn based alloys in aqueous NaCl solution, J. Magnes. Alloy. 2 (2014) 245–256. doi:10.1016/j.jma.2014.08.002.

25. A.D. King, N. Birbilis, J.R. Scully, Accurate Electrochemical Measurement of Magnesium Corrosion Rates; a Combined Impedance, Mass-Loss and Hydrogen Collection Study, Electrochim. Acta. 121 (2014) 394–406. doi:10.1016/j.electacta.2013.12.124.

26. M. Curioni, F. Scenini, T. Monetta, F. Bellucci, Correlation between electrochemical impedance measurements and corrosion rate of magnesium investigated by real-time hydrogen measurement and optical imaging, Electrochim. Acta. 166 (2015) 372–384. doi:10.1016/j.electacta.2015.03.050.